The Mathematics of Thermal Diffusion Shocks

Vitalyi Gusev[1], Walter Craig[2], Roberto LiVoti[3], Sorasak Danworaphong[4], and Gerald J. Diebold[5]
[1] *Université du Maine, av. Messiaen, 72085 LeMans, Cedex 09 France,*
[2] *Department of Mathematics McMaster University, Hamilton, Ontario, Canada L8S 4K1,*
[3] *Universita di Roma "La Sapienza", Dipartimento di Energetica, Via Scarpa, 14 – 00161 Roma,Italy*
[4] *School of Science, Walailak University, 222 Thaiburi, Thasala District, Nakorn Si Thammarat,80160, Thailand,*
[5] *Department Chemistry, Brown University, Providence, RI, USA, 02912*

Thermal diffusion, also known as the Ludwig-Soret effect, refers to the separation of mixtures in a temperature gradient. For a binary mixture the time dependence of the change in concentration of each species is governed by a nonlinear partial differential equation in space and time. Here, an exact solution of the Ludwig-Soret equation without mass diffusion for a sinusoidal temperature field is given. The solution shows that counter-propagating shock waves are produced which slow and eventually come to a halt. Expressions are found for the shock time for two limiting values of the starting density fraction. The effects of diffusion are shown on the development of the concentration profile in time and space are found by numerical integration of the partial integration of he nonlinear differential equation.

I. Introduction

The separation of liquid mixtures in a thermal gradient was discovered by Ludwig[1] in 1856, and was described theoretically somewhat later by Soret[2]. The separation of mixtures by a thermal gradient takes place not only in liquids, but also in gases and solids as is described by nonequilibrium thermodynamics[3–6]. Recently, a new method of producing the Ludwig-Soret effect has been introduced where crossed laser beams produce thermal gradients[7–10]. The method relies on interference in the electric fields of two phase coherent light beams to write an optical grating in a weakly absorbing liquid mixture. At the nodes of the electric field, there is no absorption, while at the antinodes heat is deposited resulting in a temperature field that is sinusoidal in space[11]. A probe laser is directed at the grating at the Bragg angle, and produces diffracted beams in response to either a periodic change in absorption or by a periodic change in index of refraction that forms in the mixture as a result of thermal diffusion. A recording of the intensity of the diffracted beam gives the time development of separation of the components of the mixture.

Here we discuss solution of the Ludwig-Soret equation in a one-dimensional geometry for a sinusoidal temperature distribution. A derivation of an exact solution of the Ludwig-Soret problem with negligible mass diffusion is given in Section II. The time development of the shock fronts[12] are given in Section III. Section IV gives an expression for the shock velocity and expressions for the shock formation time for two limiting cases of the starting dentsity fraction. The effects of diffusion are shown through numerical solutions to the Ludwig-Soret equation. Derivation of the concentration profile in space at long times is given.

II. Solution to the Thermal Diffusion Equation

Thermal diffusion in a binary mixture is governed by the coupled differential equations [4]

$$\rho c_P \frac{\partial T}{\partial t} = \boldsymbol{\nabla} \cdot (\lambda \boldsymbol{\nabla} T + \kappa \boldsymbol{\nabla} c_1) \quad (1)$$

$$\frac{\partial c_1}{\partial t} = \boldsymbol{\nabla} \cdot (c_1 c_2 D' \boldsymbol{\nabla} T + D \boldsymbol{\nabla} c_1) \ , \quad (2)$$

where t is the time, ρ is the solution density, c_P is the specific heat capacity, λ is the thermal conductivity, T is the temperature above ambient, κ is a constant, D' is the thermal diffusion coefficient, D is the mass diffusion coefficient, and c_1 and c_2 are density fractions of the species that make up the solution. Since the total mass of the solution is the sum of the masses of the two components of the mixture, the densities of the two species satisfy the relation $\rho_1 + \rho_2 = \rho$, where ρ_1 and ρ_2 are the densities of the two components and ρ is the density of the mixture. If the expression relating the densities of the two species is divided by ρ, the result is an expression for the density fractions c_1 and c_2 of each of the components which obey the relation $c_1 + c_2 = 1$. The first term on the right hand side of Eq. 1 is the Fourier law for heat conduction; the second describes the Dufour effect, which refers to production of a temperature change as a result of imposition of a concentration gradient. The first term on the right hand side of Eq. 2 describes thermal diffusion, while the second describes mass diffusion.

Consider a temperature field of the form $T = T_0[1 + \sin(Kx)]$, where $2T_0$ is the peak temperature, K is a wavenumber determined by the optical fringe spacing in the grating, and x is the coordinate. If the Dufour effect is taken as negligible [4], then Eq.2 becomes

$$\frac{\partial c(z,t)}{\partial \tau} = \alpha \frac{\partial}{\partial z}\{c(z,t)[1 - c(z,t)]\cos z\} + \frac{\partial^2 c(z,t)}{\partial z^2}, \quad (3)$$

where c_2 has been written in terms of c_1, and the subscript 1 dropped from the density fraction c_1, where the thermal diffusion factor α, is defined as $\alpha = D'T_0/D$, and the dimensionless quantities τ and z are defined by $\tau = K^2Dt$, and $z = Kx$. If the last term in Eq. 3 describing diffusion is ignored, then the differential equation of motion for $c(z,t)$ can be written

$$\frac{\partial c}{\partial \tau} = -\frac{\partial f}{\partial z}, \tag{4}$$

where a "flux" $f(c,z)$ is defined as

$$f(c,z) = -\alpha c(1-c)\cos z$$

and τ is given by $\tau = K^2D$. Equation 4 is the differential form of a conservation equation that expresses the buildup of c in a volume as a consequence of a flux change in space. Since for a periodic temperature field the density fraction must also be periodic in z, it follows that $c(2\,\pi,\tau) = c(0,\tau)$. Integration of Eq. 4 over one period of the temperature field, *i.e.* from $z = 0$ to $z = 2\pi$, gives the integral form of Eq. 4 as

$$\int_0^{2\pi} c(z,t)\,dz = 2\pi c_0, \tag{5}$$

where c_0 is the density fraction at time $t = 0$, assumed to be a constant throughout the cell. The integral for the density fraction over z expresses simple mass conservation for the Ludwig-Soret effect.

The Eulerian description of the profile $c = c(z,\tau)$ by Eq. 3 can be transformed[13] into a Lagrangian description yielding the coupled pair of ordinary differential equations,

$$\frac{dz}{d\tau} = \frac{\partial f(c,\beta)}{\partial c} = \alpha(2c-1)\cos z \tag{6}$$

$$\frac{dc}{d\tau} = -\frac{\partial f(c,\beta)}{\partial \beta} = -\alpha c(1-c)\sin z, \tag{7}$$

that determine the motion of points with coordinates $z = z(\tau, c_0, z_0)$ and $c = c(\tau, c_0, z_0)$ on the zc plane for a point initially at (c_0, z_0) at time $\tau = 0$. As discussed in Ref. [13], Eqs. 6 and 7 form a Hamiltonian system of equations as found in classical mechanics, with the flux function in the present problem taking on the role of the Hamiltonian function in classical mechanics. Numerical integration of Eqs. 6 and 7 can be used to give the z coordinate and the value of c as a function of time for any point initially at (z_0, c_0), as shown in Fig. 1. Since the temperature field has a period of 2π, the solutions to Eq. 3 must also have the same periodicity. As can be seen from Fig. 1, the points $-\pi/2$ and the point $3\pi/2$ represent cold points of the grating so that the solutions to Eq. 3 are identical at these points, and for any points displaced from these points by a multiple of 2π. From

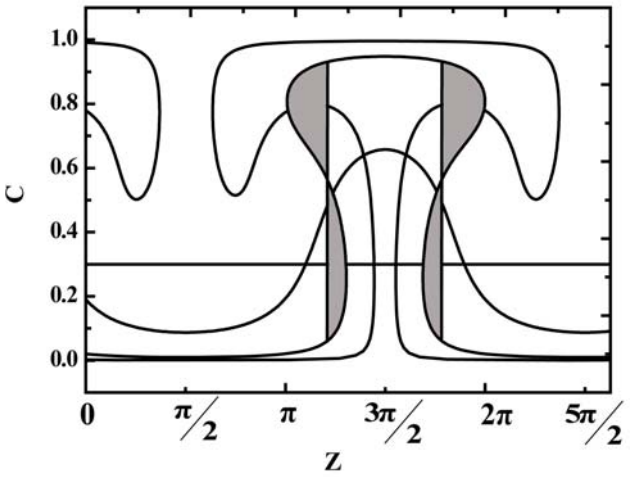

FIG. 1: Density fraction c versus dimensionless distance z for $\tau' = 0$, 1.5, 3.5, and 6.0, for a starting density fraction $c_0 = 0.3$. The curves can be determined by numerical integration of Eqs. 6 and 7 or through solution of Eqs. 12 and 13. The vertical lines indicates the positions of the shock fronts. The shock velocity is found by determining the line that makes the areas of the darkened regions adjacent to each of the vertical lines equal.

Eqs. 6 and 7 the slope of the curves on a phase portrait is found to be

$$\frac{dc}{dz} = \frac{c(1-c)\sin z}{(2c-1)\cos z},$$

which can be written as

$$\frac{d}{dz}[c(1-c)\cos z] = 0. \tag{8}$$

It follows then that the quantity in brackets in Eq. 8 is a constant, taken here to be k_1, so that

$$c(1-c)\cos z = k_1. \tag{9}$$

The phase portrait for the Ludwig-Soret equation, as shown in Fig. 2, gives the trajectories of points with specified starting values of c and z.By differentiation of Eq. 9 with respect to c, it can be seen that the maximum value of the left hand side occurs when $\cos z = 1$, and $c = 1/2$; hence the values of $k_1$are restricted to $|k_1| \le 1/4$.

By solving Eq. 7 and Eq. 9 for $\sin z$ and $\cos z$, respectively, squaring and adding the resulting expressions, it is easily shown that

$$\left[\frac{k_1}{c(1-c)}\right]^2 + \left[\frac{1}{c(1-c)}\right]^2 \left(\frac{dc}{d\tau'}\right)^2 = 1,$$

which can be written

$$\frac{dc}{\sqrt{c^2(1-c)^2 - k_1^2}} = \pm d\tau'. \tag{10}$$

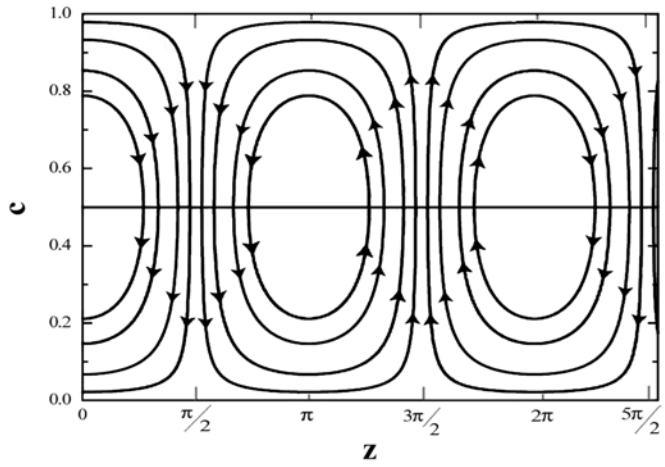

FIG. 2: Phase portrait for the density fraction c versus dimensionless distance along the grating z from Eq. 9. Points on the zc plane move along curves of constant k_1 as time progresses.

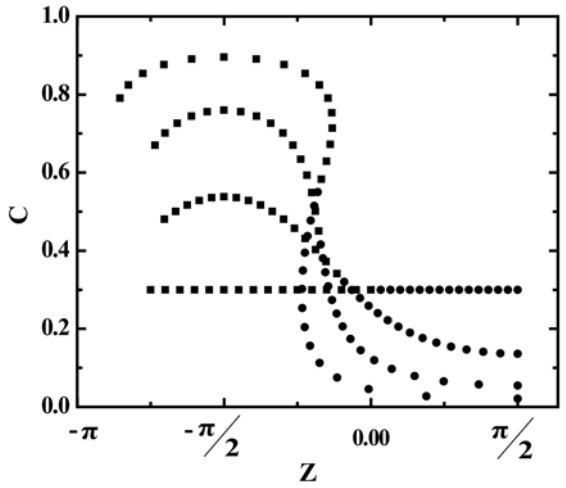

FIG. 3: Density fraction c versus dimensionless distance z from Eq. 16. with $\alpha = 1$ for $\tau' = 0$, 1, 2,and 3. 0. The points plotted as dots (•) are those that originally lie in the region $0 < z < \pi/2$ at $\tau' = 0$. The points plotted as squares (■) are those that lie in the region $-\pi/2 < z < 0$ at time $\tau' = 0$.

It is convenient to define the departure of the density fraction from a value of 1/2 through the variable c', and to express the quantity in the denominator of Eq. 10 in terms of two parameters a and b, defined by

$$c' = c - \frac{1}{2}$$

$$a = \sqrt{\tfrac{1}{4} + k1} \quad b = \sqrt{\tfrac{1}{4} - k1}\,.$$

Owing to the restriction on the magnitude of k_1, the inequality $a \geq b \geq 0$ is automatically satisfied. Hence, Eq. 10 then can be integrated from a starting density fraction c_0 at time $\tau' = 0$ along a curve of constant $k_1$to a density fraction c at time τ'giving

$$\int_{c_0-\frac{1}{2}}^{c-\frac{1}{2}} \frac{dc'}{\sqrt{(a^2 - c'^2)(b^2 - c'^2)}} = \pm \int_0^{\tau'} d\tau'', \qquad (11)$$

where the integration is taken over a trajectory in phase space with a constant value of k_1. The left hand side of Eq. 11 can be expressed as an elliptic integral[14] of the first kind F, so that the solution to the Ludwig-Soret problem for a sinusoidal temperature field, neglecting diffusion is

$$F\left[\arcsin \frac{c-\frac{1}{2}}{\sqrt{\frac{1}{4}-k_1}}, \frac{\frac{1}{4}-k_1}{\frac{1}{4}+k_1}\right] - F\left[\arcsin \frac{c_0-\frac{1}{2}}{\sqrt{\frac{1}{4}-k_1}}, \frac{\frac{1}{4}-k_1}{\frac{1}{4}+k_1}\right] = \pm\tau'\sqrt{\tfrac{1}{4}+k1}\,. \qquad (12)$$

It can be seen that Eq. 12 gives τ' explicitly for any starting point (z_0, c_0) that arrives at the newpoint c; the new coordinate z is determined through

$$c_0(1-c_0)\cos z_0 = c(1-c)\cos z = k_1. \qquad (13)$$

From the point of view of calculating density fraction profiles as shown in Fig. 1, it is convenient to specify values of z_0, c_0 and τ' and to solve Eq. 12 for the new values of c through a numerical root search. Alternately, the points (c, z) can be substituted directly into Eq. 12 through use of Eq. 13 to determine k_1. Note that for positive values of α, the minus sign is used in Eq. 12 for points moving in the hot regions of the grating $0 < z < \pi$, and the plus sign is used for motion in the cold regions $\pi < z < 2\pi$, or $-\pi < z < 0$. Inversion of Eq. 12 to give c explicitly as a function of z for any given time τ', does not appear to be possible; however it is straightforward to determine the profiles of the density fraction versus coordinate through numerical methods.

III. Motion of the Points in Phase Space

Consider the motion of a point located between 0 and $\pi/2$ with a value of $c_0 < 1/2$. It can be seen from Fig. 1 that points in this region move downwards and towards the c axis. For such points the motion is determined first by Eq. 12 with a negative sign is used, and after passing the c axis at $z = 0$, by Eq. 12 with the positive sign. Any point in this region starting at (c_0, z_0) reaches its minimum value $c_{\min}$ at $z = 0$, which from Eq. 13, is given by

$$c_{\min} = \frac{1}{2} - \sqrt{\frac{1}{4} - c_0(1-c_0)\cos z_0}. \qquad (14)$$

The time required to arrive at $c_{\min}$ is therefore

$$\tau'_{\min} = -\int_{c_0}^{c_{\min}} \frac{dx}{\sqrt{x^2(1-x)^2 - [c_0(1-c_0)\cos z_0]^2}}, \quad (15)$$

and the total time τ', from the starting point to the point (c, z) is

$$\tau' = \tau'_{\min} + \int_{c_{\min}}^{c} \frac{dx}{\sqrt{x^2(1-x)^2 - [c_0(1-c_0)\cos z_0]^2}}. \quad (16)$$

which can be written in terms of elliptic integrals as in Eq. 12. Since the shocks in the region $-\pi/2 < z < 0$ originate from points in the region $0 > z < \pi/2$, Eq. 12 is expression that determines the time of shock formation.

Similar reasoning gives the maximum density fraction $c_{\max}$ for any point starting at (c_0, z_0) located between 0 and $\pi/2$ as

$$c_{\max} = \frac{1}{2} + \sqrt{\frac{1}{4} - c_0(1-c_0)\cos z_0}, \quad (17)$$

where $\tau'_{\max}$, the time it takes to move from c_0 to $c_{\min}$ to $c_{\max}$, is given by

$$\tau'_{\max} = \tau'_{\min} + \int_{c_{\min}}^{c_{\max}} \frac{dx}{\sqrt{x^2(1-x)^2 - [c_0(1-c_0)\cos z_0]^2}}. \quad (18)$$

The curves in Fig. 3 show how points originally in the region between 0 and $\pi/2$ move downwards to their minimum values at $z = 0$, pass to the left of the c axis and then rise upwards as time progresses.

IV Shock Formation

A. Determination of the shock velocity

It is clear from examination of Fig. 2 that the solutions to Eq. 12 exhibit nonfunctional behavior after a certain time. Similar solutions for different values of c_0 show that nonfunctional behavior is found for any value of c_0 if τ' is allowed to become large. When the slope of any curve becomes unbounded, *i.e.*. immediately before the density fraction profile becomes nonfunctional, shocks are formed, and the mathematics must be treated in a different manner.

Consider the vertical line to the right of the density fraction maximum at $3\pi/2$ indicating the position of the shock front on the curve in Fig. 1 for $\tau' = 3.5$. For the shock front, the density fraction immediately to the left of the front is denoted c_l and that to the right of the shock by c_r. The area of the curve bisected by the vertical line, can be equated to the product of the velocity of the shock $dz_{sh}/d\tau$, the difference in c and the time interval $d\tau$,that is,

$$\frac{dz_{sh}}{d\tau}(c_l - c_r)d\tau = \int_{c_r}^{c_l} dz\, dc,$$

which, together with Eq. 6, gives

$$\frac{dz_{sh}}{d\tau}(c_l - c_r)d\tau = \alpha \cos z\, d\tau \int_{c_r}^{c_l} (2c-1)\, dc. \quad (19)$$

After evaluation of the integral in Eq. 19 the shock velocity becomes

$$\frac{dz_{sh}}{d\tau} = \alpha(c_l + c_r - 1)\cos z. \quad (20)$$

It can be seen that two shocks, one on either side of the point $z = 3\pi/2$ are formed, each of which travels with the same speed towards the cold region of the grating, the different velocities being determined by the change in sign of the cosine function on either side of $z = 3\pi/2$. The left-going shock comes to a halt when $c_l = 1$ and $c_r = 0$, that is, where a complete separation of the mixture has been attained, at which point the profile of c in space is a square wave centered at $z = 3\pi/2$.

The shock velocity can be obtained equally by writing Eq. 6 as $dz_{sh}/d\tau = [f(c_l, z) - f(c_r, z)]/(c_l - c_r)$, which, after substitution of the expression for the flux function, gives Eq. 20. As noted in Ref. [12], Eq. 20, which expresses the thermal diffusion shock velocity in terms of density fractions on either side of the shock, is an exact analog of the Rankine-Hugoniot relations for one-dimensional fluid shocks: Eq. 20 gives the thermal diffusion shock speed in terms of the "state variables" c_l and c_r, the Rankine-Hugoniot relations express the shock speed in terms of ratios of the state variables of the fluid on either side of the shock.

The time of formation of the shock can be found from numerical integration of the Hamiltonian system of equations and finding the point in space and time where the profile reverses direction. Figure 4 shows a plot of the dimensionless time τ' required for shock formation versus the initial density fraction c_0 found from Eqs. 6 and 7. Determination of a general expression for the time of shock formation in closed form is difficult; however, solutions for two limiting cases, $c \lesssim c_0$, and $c_0 \cong 0$ can be found.

B. Shock formation time: $c_0 \lesssim 1/2$

Consider the region between $-\pi/2$ and $\pi/2$. When c_0 is approximately equal to $1/2$, the shock must form at a point to the left of the c axis, but near the point $z = 0$. If the cosine function is approximated as $\cos z \cong 1 - z^2/2$ and substituted into Eq. 9 then the profiles of shown in

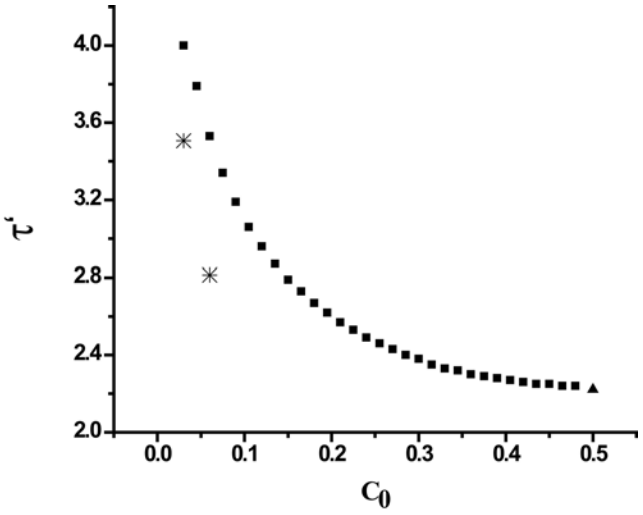

FIG. 4: Time for formation of a shock τ' versus the starting density fraction c_0 from numerical integration of the Hamiltonian system of equations. The point (▲) at $c_0 \cong 1/2$, is the limining value of τ' from Eq. 28. The points (∗) are from Eq.30for $c_0 \ll 1$

Fig. 1 reduce to circles described by

$$\left(\frac{z}{2\sqrt{2}}\right)^2 + c'^2 = \frac{1}{4} + k_1 \tag{21}$$

on the zc plane for $k_1 \geq -\frac{1}{4}$. Substitution of z from Eq. 21 into Eq. 7 with the sine function approximated as $\sin z \cong z$ gives,

$$\frac{dc'}{\sqrt{\frac{1}{4} + k_1 - c'^2}} = \pm d\tau', \tag{22}$$

which can be integrated to give

$$\arcsin\left(\frac{c'}{\sqrt{\frac{1}{4}+k_1}}\right) - \arcsin\left(\frac{c'_0}{\sqrt{\frac{1}{4}+k_1}}\right) = \frac{\tau'}{\sqrt{2}}. \tag{23}$$

Further manipulation of Eq. 23 gives for $z < 0$

$$\frac{c'\sqrt{c'^2 - c'^2_0 + z^{\dagger 2}} + c'_0 z^\dagger}{c'^2 + z^{\dagger 2}} = \sin\tau^\dagger, \tag{24}$$

where $z^\dagger$ has been defined as $z^\dagger = z/2\sqrt{2}$ and $\tau^\dagger = \tau'/\sqrt{2}$. It is convenient at this point to express the coordinates c' and $z^\dagger$ in Eq. 24 in cylindrical coordinates, $c' = -r\cos\phi$ and $z^\dagger = -r\sin\phi$, where ϕ is an angle measured clockwise with respect to the negative c axis Equation 24 gives, after some algebraic manipulation,

$$r = -c'_0 \frac{\cos(\phi + \tau^\dagger)}{\cos^2\phi - \sin^2\tau^\dagger} \tag{25}$$

for points in the region $-\pi/2 \leq z \leq 0$. The modified density fraction $c'$and coordinate $z^\dagger$ then become

$$\begin{aligned} z^\dagger &= c'_0 \frac{\cos(\phi+\tau^\dagger)}{\cos^2\phi - \sin^2\tau^\dagger}\sin\phi \\ c' &= c'_0 \frac{\cos(\phi+\tau^\dagger)}{\cos^2\phi - \sin^2\tau^\dagger}\cos\phi. \end{aligned} \tag{26}$$

The condition for the appearance of a shock is that $dz^\dagger/dc'$ should approach zero, which from Eqs. 26 can be found as

$$\frac{dz^\dagger}{dc'} =$$

$$\frac{\cos(2\phi+\tau^\dagger)[\cos^2\phi - \sin^2\tau^\dagger] + \sin(2\phi)\cos(\phi+\tau^\dagger)\sin\phi}{\sin(2\phi)\cos(\phi+\tau^\dagger)\sin\phi - \sin(2\phi+\tau^\dagger)[\cos^2\phi - \sin^2\tau^\dagger]} \tag{27}$$

The shock for c'_0 approximately equal to zero is expected to appear at $\phi = \pi$ so that Eq. 27 reduces to $dz^\dagger/dc' = -\cot\tau^\dagger = 0$; hence, it follows that $\tau^\dagger = \pi/2$, for the time of shock generation, and the time for shock formation is

$$\tau' \simeq \frac{\pi}{\sqrt{2}}. \tag{28}$$

As can be seen in Fig. 4 the shock time given by Eq. 28 is in excellent agreement with the numerical results.

C. Shock formation time: $c_0 \cong 0$

A second case where the time of shock formation time can be found in closed form is when the initial density fraction is small. Consider points in the region $-\pi/2 < z < \pi/2$. Starting from Eq. 16, the time for the density fraction to reach a value c starting from the point (z_0, c_0) can be shown to be given by

$$\begin{aligned} \tau' = &\int_{c_0}^{c} \frac{dx}{\sqrt{x^2(1-x)^2 - c_0^2(1-c_0)^2\cos^2 z_0}} \\ &+2\int_{c_{\min}}^{c_0} \frac{dx}{\sqrt{x^2(1-x)^2 - c_0^2(1-c_0)^2\cos^2 z_0}}. \end{aligned} \tag{29}$$

It is clear from plots found from the solution to Eq. 16 or through numerical integration of Eqs. 6 and 7, that the points first forming the shock lie originally in the region $0 < z < \pi/2$ and which move downward and to the left along the curves shown in Fig. 2. For small c_0, the shock forms at values of $c \simeq 1/2$ near $-\pi/2$ from points z_0 on the positive z axis where $z_0 \simeq 0$. Equation 29 can then be approximated as

$$\tau' \simeq \int_{c_0}^{1/2} \frac{dx}{\sqrt{x^2 - c_{\min}^2}} + 2\int_{c_{\min}}^{c_0} \frac{dx}{\sqrt{x^2 - c_{\min}^2}}$$

giving τ' as

$$\tau' \simeq -\ln c_0 + \ln\left(\frac{c_0 + \sqrt{c_0^2 - c_{\min}^2}}{c_{\min}}\right)$$

where $c_{\min} \simeq c_0 \cos z_0$. The time for the shock to form for small c_0 is thus

$$\tau' \simeq -\ln c_0 \tag{30}$$

The plot in Fig. 4 gives two points from Eq. 30. Evaluation of the shock time for values smaller than those given in Fig. 4 shows that the approximation given by Eq. 30 gets successively better for small values of c_0. For example, for $c_0 = 5 \times 10^{-5}$, numerical integration gives τ'=10.6 whereas Eq. 30 gives $\tau' = 9.9$

V. Effects of Mass Diffusion

A. Results from numerical integration

The effects of mass diffusion were determined by numerical integration of Eq. 3 using the finite difference method, which gives a solution by considering small changes in the density fraction resulting from a change in time $\Delta\tau$ and space Δz. A solution for c is obtained by selecting successively smaller values of $\Delta\tau$ and Δz until the solution converges. The first order derivative of the density fraction with respect to z at a time t_k at the point z_k is given, for instance, by

$$\frac{\partial c}{\partial z} = \frac{c(t_k, z_{i+1}) - c(t_k, z_{i-1})}{2\Delta z}. \tag{31}$$

Since derivatives must be computed at the end points of the integration range in space, the periodicity of the solution is used to give values for the required derivatives. The modulus function, $\mathrm{mod}(a, b)$, is introduced to represents the remaining integer of division of a by b. For example, $\mathrm{mod}(3, 2)$ is equal to one and $\mathrm{mod}(4, 2)$ is equal to zero. If a is less than b, the value of the modulus function is a, where a is a positive integer, including zero. The expressions for the first and second space derivatives become

$$\frac{\partial c}{\partial z} = \frac{c(t_k, z_{\mathrm{mod}(i+1,i_{\max})}) - c(t_k, z_{\mathrm{mod}(i-1,i_{\max})})}{2\Delta z}$$
$$\frac{\partial^2 c}{\partial z^2} = \frac{c(t_k, z_{\mathrm{mod}(i+1,i_{\max})}) - 2c(t_k, z_i) + c(t_k, z_{\mathrm{mod}(i-1,i_{\max})})}{\Delta z^2}$$

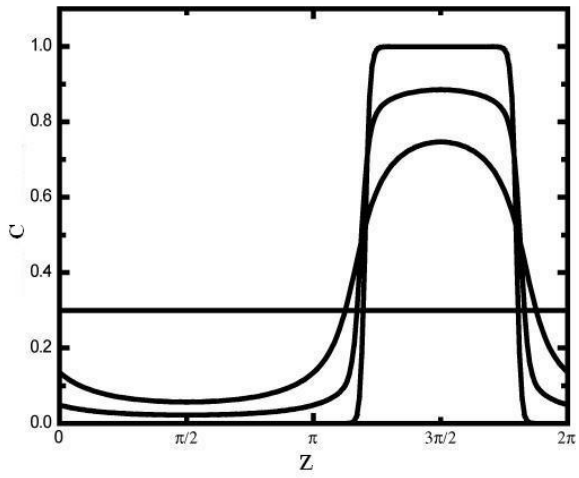

FIG. 5: Density fraction c versus dimensionless distance z for α=40. The times for the plots are $\tau' = 0$, 0.20, 0.40, and1.08 for plots with successively higher peak values of c

To simplify the notation, z_i and τ_k are now replaced by their indices, giving Eq. 3 as

$$c(k+1,i) = c(k,i) + \alpha_T \Delta\tau \cos(2\pi \frac{i}{i_{\max}})(1 - 2c(k,i)) \tag{32}$$
$$\left[\frac{c(k, \mathrm{mod}(i+1, i_{\max})) - c(k, \mathrm{mod}(i-1, i_{\max}))}{2\Delta z}\right]$$
$$-\alpha_T \Delta\tau \left[\sin(2\pi \frac{i}{i_{\max}})(c(k,i) - c^2(k,i))\right] + \left(\frac{\Delta\tau}{\Delta z^2}\right) \times$$
$$[c(k, \mathrm{mod}(i+1, i_{\max})) - 2c(k,i) + c(k, \mathrm{mod}(i-1, i_{\max}))].$$

The plots shown in Fig. 5 indicate that the effect of diffusion is to remove the high spatial frequencies in the distribution. Since the spatial profile of c depends on α and τ' only, it is possible to calculate the spatial Fourier components of the distribution after obtaining c from numerical integration, and hence to determine the intensity of light diffracted from an absorption grating, as was done in Ref. [12]. By minimizing the error in a fit to the intensities of the diffracted light beams, the thermal diffusion factor can be determined from experimental data.

B. Density fraction distribution for long times

When τ' becomes long, thermal diffusion is exactly balanced by mass diffusion and the spatial profile of the density fraction must approach a limiting form. It can be seen that when $dc/d\tau' = 0$, Eq. 3 reduces to an ordinary differential equation in z, a first integral of which is given by

$$\frac{dc}{dz} + \alpha c(1-c)\frac{d\hat{T}}{dz} = C, \tag{33}$$

where C is a constant, and a dimensionless spatial derivative of the temperature field $d\hat{T}/dz$ has been substituted for the cosine function. For temperature fields that are periodic in z it is expected that in the region $0 < z < 2\pi$, both dc/dz and $d\hat{T}/dz$ will be zero at the some value of z. For the present problem, both of these quantities are zero at the point $z = 3\pi/2$; hence the constant C must be zero and Eq. 33 can be integrated as

$$\int_{c(z_0)}^{c(z)} \frac{dc}{c(1-c)} = -\alpha \int_{z_0}^{z} \frac{d\hat{T}}{dz} dz. \tag{34}$$

The general solution to 34 is thus,

$$c(z) = \frac{1}{1 + Fe^{\alpha T(z)}} \tag{35}$$

where F is a constant given by $[1 - c(z_0)] \exp[-\alpha \hat{T}(z_0)]/c(z_0)$ For the present problem with a sinusoidal temperature field, the long time distribution becomes

$$c(z) = \frac{1}{1 + Fe^{\alpha \sin z}}. \tag{36}$$

An equivalent expression for the linearized Eq. 3 has been given in Ref. [13]. Since the value of $c(z_0)$ is not known without solution to Eq. 3, $F(\alpha, c_0)$ can be determined for a given value of α and c_0 through use of the mass conservation law, Eq. 5. Depending on the value of α, curves of c versus α from Eq. 36 can resemble a sinusoidal function for small α, or a nearly square wave for large α.

VI. Discussion

The expressions in Eqs. 12 and 16 provide an exact solution to the thermal diffusion problem without mass diffusion. If Eq. 3 is divided by α so that the time derivative is expressed with respect to τ', it is clear that the effects of diffusion are small when α is large or when the gradient of the density fraction is small, such as at short times. The conditions for the time of appearance of the shocks is straightforward, however, the complexity of an explicit expression for the shock time in terms of α and c_0 appears to be great.

The formation of a shocks follows from the nonlinearity of the dependent variable c in Eq. 3. Perhaps the unique feature of shocks produced by thermal diffusion in sinusoidal temperature fields is that they come as counter-propagating pairs of waves, the direction of which is governed by the sign of the cosine function in Eq. 20 to the right and left of $z = 3\pi/2$.. The left-going wave near $z = 3\pi/2$ has the property that it slows to a speed of zero when c_l approaches one, and c_r approaches zero. At this point in time, a complete separation of the mixtures, possible only in the absence of diffusion, takes place.

The parallel between thermal diffusion shocks and fluid shocks has been given in Ref. [12]. In both cases, the mathematics are treated by ignoring the dissipative term in the equations of motion to find the properties of the shock waves. In fluid shocks, viscosity causes a broadening of the shock front, just as mass diffusion broadens the thermal diffusion shock fronts as shown by the results of numerical integration given here. The extent to which thermal diffusion shocks are visible in the laboratory is clearly a function of how large the thermal diffusion factor can be made.

ACKNOWLEDGEMENT

SD and GD acknowledge the support of the US Department of Energy, Office of Basic Energy Studies under grant ER 13235. WC acknowledges partial support for his research from the NSF under grant DMS-0070218, the NSERC under grant #238452-01, and the Canada Research Chairs Program

[1] C. Ludwig, Sitzber. Akad. Wiss. Vien Math.-naturw. **20**, 539 (1856).
[2] C. Soret, Arch. Sci. Phys. Nat. Geneve **3**, 48 (1879).
[3] D. D. Fitts, *Nonequilibrium Thermodynamics*, McGraw-Hill, New York, 1962.
[4] S. R. deGroot and P. Mazur, *Non-Equilibrium Thermodynamics*, North Holland, Amsterdam, 1962, As noted in this reference the Dufort effect is generally small and can be ignored.
[5] E. A. Mason, R. J. Munn, and R. J. Smigh, Thermal diffusion in gases, in *Advances in Atomic and Molecular Physics*, edited by D. R. Bates, page 33, New York, 1966, Academic Press.
[6] R. D. Present, *Kinetic Theory of Gases*, McGraw Hill, New York, 1958.
[7] K. Thyagarajan and P. Lallemand, Opt. Commun **36**, 54 (1978).
[8] F. Bloisi, Opt. Commun. **68**, 87 (1988).
[9] W. Köhler, J. Chem. Phys. **98**, 660 (1993).
[10] W. Köhler and S. Wiegand, Measurement of transport coefficients by an optical grating technique, in *Thermal Nonequilibrium Phenomena in Fluid Mixtures*, edited by W. Köhler and S. Wiegand, page 190, Springer Verlag, Berlin, 2001.
[11] H. J. Eichler, P. Gunter, and K. W. Pohl, *Laser-Induced Dynamic Gratings*, Springer, Berlin, 1985.
[12] S. Danworaphong, W. Craig, V. Gusev, and G. J. Diebold, submitted for publication .
[13] W. L. Craig, S. Danworaphong, and G. J. Diebold, Physical Review Letters **92**, 125901 (2004).
[14] L. M. Milne-Thompson, *Handbook of Mathematical Functions with Formulas, Graphs, and Mathematical Tables*, volume 55, page 596, National Bureau of Standards, Washington D.C., 1964, Some authors (*e.g.* I. Gradshyteyn and Ryzhik, Table of Integrals, Series, and Products, Academic Press, New York, 1980) give the elliptic

integral with the second argument as a/b instead of a^2/b^2, which we believe to be correct.